



IEA-SHC TASK 43: SOLAR RATING AND CERTIFICATION PROCEDURES

White Paper on Solar Air Heating Collectors

Date: May 2013

Author: Korbinian S. Kramer*

Participants: Fraunhofer ISE

*Based on the work of Christoph Thoma, Christian Welz, Stefan Fortuin, Stefan Mehnert, Jens Richter, Michael Hermann, Gerhard Stryi-Hipp, et al., corresponding author; korbinian.kramer@ise.fraunhofer.de

Contributing Editor: Les Nelson, International Association of Plumbing & Mechanical Officials

TABLE OF CONTENTS

1	INTRODUCTION	3
1.1	Description of work carried out	3
2	TECHNOLOGY OVERVIEW	3
2.1	Air heating collector construction and flow patterns	3
2.2	Benefits and drawbacks of air heating collectors	5
2.3	Examples of the application of air heating collectors	6
3	REVIEW OF PERFORMANCE MODELS, TESTING PROCEDURES AND STANDARDS	7
4	PERFORMANCE TEST PROCEDURES	9
4.1	Performance test procedure description for air collectors	9
4.2	Mass Flow Dependency	10
4.3	Reference temperature for the performance curve	15
4.4	Detailed work on measurement methods and leakage rate to achieve suitable accuracy	18
4.5	Comparison of two methods for temperature measurement in gas streams	20
4.5.1	<i>Method 1: Multi-temperature sensors with air blender</i>	20
4.5.2	<i>Method 2: Integrating temperature sensor with two nets</i>	22
4.5.3	<i>Effect of fine mesh nets on temperature</i>	24
4.6	Conclusions regarding measurement of air flow and temperature	25
4.7	Performance test methods for uncovered/covered, open to ambient and closed loop collectors	27
4.8	Simulation tools for different technologies and applications	29
5	AIR COLLECTOR TESTS	28
6	ANNEX: SUBTASK A ROADMAP CONTENT RELATED TO AIR HEATING COLLECTORS	29
7	REFERENCES	29

1 INTRODUCTION

1.1 Description of work carried out

Although solar air heating collectors have some significant advantages in comparison to liquid heating collectors, currently they have a market share of less than 1% (Weiss, Bergmann et al. 2009) of the global solar collector market. The main advantages of using air as heat transfer medium are the absence of stagnation and freezing problems and a reduced tightness requirement. For instance, this makes it easier to integrate solar air heating collectors into façades. Commercially available air heating collector types range from unglazed collectors for space heating support at low temperatures, to high performance evacuated tube collectors with high efficiencies at increased temperatures. An important barrier for a broader use of solar air heating collectors is the lack of common standards for testing to ascertain quality and performance. The Fraunhofer Institute for Solar Energy Systems ISE is currently working on the development of testing standards for glazed and unglazed air collectors, the development of simulation tools to calculate solar gains of solar air heating systems as well as the improvement of solar air heating collector technology. This work is done in co-operation with industry within the project ‘Luko-E’, which is co-funded by the German ministry for the environment.

2. TECHNOLOGY OVERVIEW

Different air heating collector concepts are used in different niche markets. Today’s applications include: direct use of the heated air in space heating, solar assisted air drying applications, and water heating involving the use of a heat exchanger to a secondary fluid-based heat transfer medium and storage loop [5]. Unglazed air heating collectors are mainly used in North America on large façades of commercial and public buildings to pre-heat ambient air for space heating. Glazed air heating collectors are mainly used in Europe for space heating support in commercial applications, as well as for some process heating purposes, e.g. the drying of malt at the Brauerei Lammsbräu in Germany. In addition, autonomous solar air heating collector units, typically with 2 m² of collector area and an integrated PV solar driven ventilator, are used to heat air in small buildings such as weekend houses.

2.1 Air heating collector construction and flow patterns

Air collector development focuses on improvements in the heat transfer construction due to the low thermal capacity of air and the much lower heat transfer coefficient between absorber and air, as compared with a liquid heat transfer media. An improved heat transfer coefficient can be realized by increasing the surface area that is in direct contact with the air, or ‘intensifying’ the contact itself by directing the air flow through holes in a sheet absorber (perforated absorber), or by using absorbers with very large surface areas.

Unlike with water heating collectors it is not necessary to use hermetically sealed channel structures for air heating collectors. Air as a heat transfer medium thus allows for higher flexibility in the construction, such as the position of the absorber. Many different absorber

geometries and collector flow designs can be utilized. Figure 1 shows different absorber-flow designs of air heating collectors. A1-A3 and B1-B3 are glazed; A4 and B4 are unglazed examples. Row ‘A’ shows the perforated transparent cover or perforated absorbers through which the air is passed to improve the heat transfer coefficient. A1 and A4 configurations take in fresh outside air through these holes; the absorber design is also known as “transpired.” Row ‘B’ shows glazed and unglazed air collectors where the air flows between the glazing and the absorber, behind the absorber, or on both sides of the absorber. Not shown is a possible channel or fin structure attached to the absorber, which would increase the absorber-air contact area.

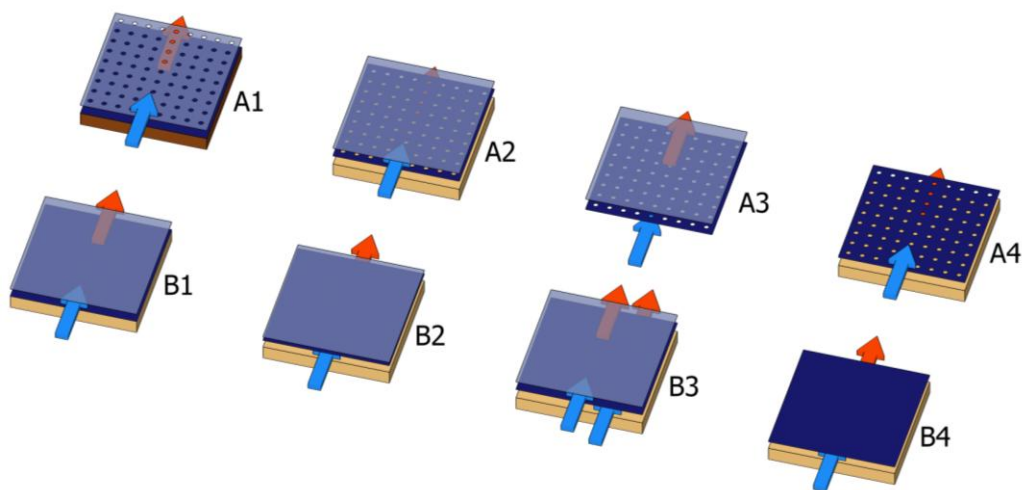


Fig.1: Different types of covered (glazed) and non-covered (unglazed) air heating cover-absorber constructions ©Fraunhofer ISE

A solar air heating collector system is called ‘open’ loop if fresh air is drawn into the collector from outdoors; where it is heated and used directly. In contrast, ‘closed’ loop air collector systems circulate the air through the system and the collector and transfer the heat via a heat exchanger to the point of usage. ‘Closed’ loop systems are able to provide higher outlet temperatures, because the inlet temperature can be higher than the ambient air. If air is drawn into the collector via an intake manifold, the collector can operate in either ‘open’ or ‘closed’ loop systems. If the ambient air is sucked in through holes in either the absorber or the glazing it can be only operated in an open system, and is therefore called ‘open to ambient collector’.

Open to ambient collectors are typically used in façades to preheat the ambient air, which is drawn into the collector and then used in a building. Since the collector operates at only a small temperature differential compared to ambient, even a small temperature increase of the ambient air provides useable heat, and the efficiency of open to ambient collectors can

be high. However, the amount of solar thermal energy which can be moved into the building is limited due to the low heat capacity of the air and the low temperature increase in the collector. Therefore the solar fraction of such an open to ambient system is usually rather small. However, since these types of air heating systems are relatively easy to design and construct, they can be very cost effective.

Closed loop collectors are usually covered collectors and operate at higher temperatures, in some cases to process heat temperatures ranges, and can be advantageous because stagnation problems are minimal in comparison to fluid-based collectors. For high temperature applications a high efficiency evacuated tube air heating collector capable of generating air temperatures up to 120°C was developed at Fraunhofer ISE [9].

However, in addition to design features that achieve good heat transfer, it is important to optimize the collector design so as to achieve a low pressure drop, which will limit the use of electricity for powering the ventilator for the forced air circulation.

2.2 Benefits and drawbacks of air heating collectors

To increase the market performance of solar air heating collectors and systems, end use applications must be identified where the drawbacks are minimized or avoided and are outweighed by the benefits. A general overview is given in Tab. 1.

Tab. 1: Benefits and drawbacks of air heating collectors

Benefits	Drawbacks
<ul style="list-style-type: none"> • No freezing or stagnation problems • Usually simpler and less expensive systems • Very efficient preheating of fresh air for buildings possible • No problems from leaks, no damage, no environmental or health hazard risk from spilled heat transfer medium (use in façades is possible) 	<ul style="list-style-type: none"> • Low heat capacity of air, thus high air volume rates and larger channels are necessary • Poor heat transfer between absorber and air • Closed loop systems: <ul style="list-style-type: none"> - Additional losses in the air-water heat exchanger - Second solar circuit required (air circuit and water circuit) • Open to ambient systems <ul style="list-style-type: none"> - Limited/low temperature range - Fan noise and open air ducts

Today, the solar air collector market is growing in niches where they are already cost effective. This is often the case for the unglazed transpired solar façades in large buildings such as warehouses and livestock buildings in North America. These buildings use outside air for space heating and often have large façades which receive significant sunshine during winter months. In some applications in central Europe, covered solar air heating collectors are competitive with liquid heating collectors. In addition, new applications are under development due to a growing share of buildings with controlled air systems in Europe where new market opportunities for solar air collector systems are expected.

The following market niches for solar air heating collectors can be identified in Europe:

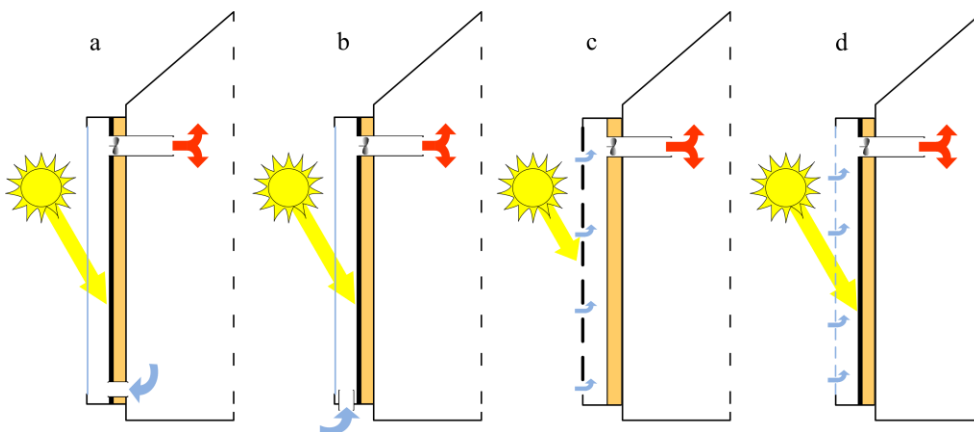
- Common single/two family houses with domestic hot water (DHW) only or combined systems for DHW and space heating support.
- Niche, applications in multi-family housing, heating of non-residential/utility buildings, process heat applications.
- Future applications in high solar fraction houses (>50% solar fraction)

2.3 Examples of the application of air heating collectors

Solar air heating collectors can be used in different ways. **Error! Reference source not found.** shows simple systems where solar heated air is used directly for space heating. In this case the façade mounted air collector heats up inside air (a) or outside air (b, c and d) and releases the hot air directly into the building. In this case the building itself is the only means for storing the heat. It is also possible to pass the heated air through a storage facility with high thermal mass to increase heat storage capacity separate from the building mass.

In some collectors a small PV panel is integrated which provides the electricity for the ventilator that drives the air flow through the collector. Since the PV panel produces electricity proportional to the solar irradiation and thus the heat produced, automatic operation is possible without the use of an additional controller.

Fig. 2. Simple air heating collector concepts



Error! Reference source not found. shows a solar ‘combi’-system for combined domestic hot water and space heating applications. The solar air heating collector is typically installed on the roof. A three way valve at the air intake allows for drawing in outside air heating the building. Alternatively, inside air can be drawn into the collector, heated, and directed back into the building in a “recirculation” mode. ©Fraunhofer ISE

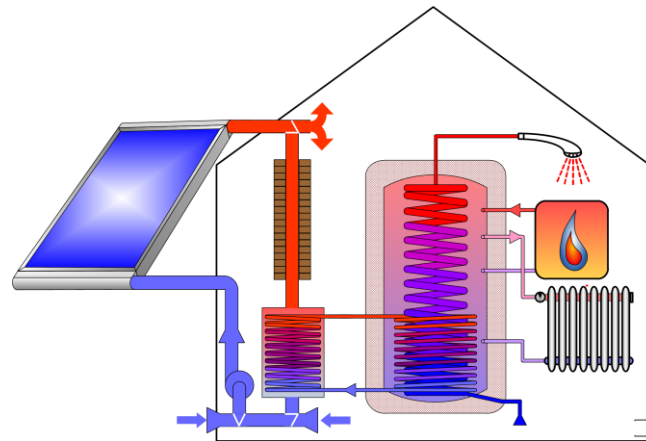


Fig. 3: Example of a solar “combi-system” using an air heating solar collector.

For direct use of the heated air throughout the building, the distribution via air channels that are large in comparison to the pipes in the water heating circuit is necessary. Alternatively, a so called hypocaust heat storage system can be installed, where the heated air flows through channels in walls and floors, which take up the heat and slowly release it into the building. If there is no immediate need for direct heating in the building, the heat can be stored in a conventional water storage tank via an air-water heat exchanger. ©Fraunhofer ISE

3 REVIEW OF PERFORMANCE MODELS, TESTING PROCEDURES AND STANDARDS

Common testing standards are a basic requirement to develop a market, since only with common standards can the quality of the components be certified, the performance measured, the solar yield calculated accurately, and the performance of the components compared. This information helps identify product improvements and drives competitive market growth. However, current testing standards do not yet sufficiently cover solar air heating collectors, at least from the European point of view.

The oldest and most well-known air heating collector standard is the ANSI/ASHRAE 93, first published in 1977. This standard is periodically revised and updated by the American Society of Heating, Refrigerating and Air-Conditioning Engineers, most recently in 2010. ANSI/ASHRAE 93 provides a good basis for measuring the performance of solar air heating collectors, however durability and reliability tests are not included in the standard. Since 2010, the Test Lab for Solar Thermal Systems at the Fraunhofer ISE has been accredited for this standard.

Currently, no European test standard for solar air heating collectors is available. The existing solar collector test standard EN 12975:2006 does not cover solar air heating collector technologies. In Germany, solar collectors require a Solar Keymark certification

based on a test performed according to EN 12975 to be eligible for subsidies. However, since there is no EN test standard available yet, as an interim solution solar air heating

collectors tested according to the relevant parts of EN 12975 are accepted for subsidies as long as no new framework is established. This has caused and will likely cause more problems among manufacturers competing with slightly different solar air heating technologies, some of which can be tested, certified and subsidised, and some which cannot.

To remedy this situation, and to create a uniform system of test standards, a draft extension to the EN 12975 standard for covered solar air heating collectors was developed by Fraunhofer ISE and proposed to the standardization committees at the end of 2010. The text is based on the ANSI/ASHRAE 93 standard, but was further developed. Since the end of 2012 the draft has been in the comment phase, and is expected to be finally approved as a part of the new EN 12975, EN ISO 9806 respectively in spring 2014, latest.

In many respects, solar air heating collectors can be tested in the same way as water heating collectors. The rainwater penetration, exposure, high-temperature resistance, external thermal shock, mechanical load and stagnation temperature tests as well as the final inspection can be applied in the same way as for water heating collectors.

However, some durability and reliability tests have to be modified for solar air heating collectors, including the thermal performance test, determination of the Incident Angle Modifier (IAM), determination of collector capacitance, the internal thermal shock test and the internal pressure test.

The pressure drop test for water heating collectors is optional, however for air heating collectors it should be mandatory. Unlike water heating collectors, an air heating collector is usually not fully air tight. Therefore the classical tightness test is not appropriate. Since the leakage rate has a strong influence on the collector performance, it must be taken into account in the performance evaluation and therefore must be measured. In addition, the determination of the maximum start temperature is mandatory for solar air heating collectors, but not considered relevant for water heating collectors.

In parallel to the European activities, the CSA F378.2 standard for solar air heating collectors was developed and published in Canada in 2011. It is also based mainly on the ANSI/ASHRAE 93 standard, but with several added functional test details, similar to the European EN 12975 standard. An overview of which tests are covered by the three standards is given in Tab. 2. The CSA F378.2 standard supports the convergence of the "American" and "European" method.

Tab. 2: Standards and tests for solar air heating collectors

	pr EN 12975-1: 2011	ANSI ASHRAE 93, 2003	CSA F 378.2, 2011	EN ISO 9806:2014
Thermal Performance				
1) Thermal Efficiency	✓	✓	✓	✓
2) Incident Angle Modifier	✓	✓	✓	✓
3) Collector Capacity	✓	✗	✗	✓
4) Collector Time Constant	✓	✓	✓	✓
Durability and Reliability Tests				
1) Internal Pressure	✓	✗	✓	✓
2) High-Temperature Resistance	✓	✗	✓	✓
3) Exposure	✓	✗	✓	✓
4) External Thermal Shock	✓	✗	✓	✓
5) Internal Thermal Shock	✓	✗	✗	✓
6) Rain Penetration	✓	✗	✗	✓
7) Mechanical Load	✓	✗	✓	✓
8) Stagnation Temperature	✓	✗	✗	✓
9) Maximum Start Temperature	✓	✗	✗	✓
10) Leakage Test	✓	✓	✓	✓
11) Pressure Drop	✓	✓	✓	✓
12) Final Inspection	✓	✓	✓	✓

The draft EN 12975 extension for air heating collectors is limited to covered collectors, since the test method for non-covered air heating collectors is not fully developed yet. However, Fraunhofer ISE is working on a subsequent draft extension, which was presented to the standardization committees at the end of 2011. Table 3 shows which collector types are covered by which standard.

Tab. 3: Solar collector types addressed by various standards

	pr EN 12975-1: 2011	ANSI ASHRAE 93, 2003	CSA F 378.1,2, 2011	EN ISO 9806:2014
Water Collectors				
Covered	✓	✓	✓	✓
Uncoverd	✓	✗	✓	✓
Solar Air Heaters Open to Ambient				
Covered	✓	✓	✓	✓
Uncoverd	✓	✗	✓	✓
Solar Air Heaters Closed Loop				
Covered	✓	✓	✓	✓
Uncoverd	✓	✗	✓	✓

As can be seen in Tables 2 and 3, the EN ISO 9806 standard is mentioned as a goal for a worldwide, unified solar air heating standard. Some important steps to achieve this goal have already been described. A joint working group of ISO and CEN under the Vienna Agreement has taken up this topic. A unified CEN-ISO standard for solar air heating collectors is ready to be published for comments and could be approved in 2013. Fraunhofer ISE is supporting this process actively with the development of the missing parts of the standard.

4 PERFORMANCE TEST PROCEDURES

4.1 Performance test procedure description for air collectors

To measure collector performance with high accuracy and repeatability is a must for further developing the solar system market. Only a well-defined performance test allows for comparison of collectors' performance, allows the calculation of the yield of solar

systems, and stimulates constructive competition and innovations. In addition, it is a requisite for gaining a deeper understanding of the technology and the research work needed to improve the technology.

Requirements for testing include unambiguous methodology and precise test equipment, as well as definitions of what must be measured under what conditions, and the content and formatting of the results. Solar air heating collectors have some peculiarities which dictate differences in some aspects of performance testing as compared with that of liquid based collectors. The most important differences are presented in the following.

The results of this work were the basis for the draft extension for solar air heating collectors, which is currently in the comment phase of EN 12975.

For covered solar liquid heating collectors the following performance model for instantaneous efficiency is broadly used:

$$\eta = \eta_0 - a_1 \frac{T_m - T_a}{G} - a_2 \frac{(T_m - T_a)^2}{G} \quad (\text{eq. 1})$$

With the maximum efficiency:

$$\eta_0 = F' \cdot (\tau\alpha)_{eff} \quad (\text{eq. 2}),$$

And the mean temperature of the heat transfer medium:

$$T_m = \frac{1}{2} (T_{in} + T_{out}) \quad (\text{eq. 3})$$

With the ambient temperature (T_a), the inlet and outlet temperature of the heat transfer medium (T_{in} , T_{out}), the transmission of the cover (τ), the absorption of the absorber (α), the collector efficiency factor (F') and the solar radiation (G). The collector efficiency is determined with the parameters: η_0 , a_1 , a_2 .

4.2 Mass flow dependency

The most important difference between liquid and air collectors is the much lower heat transfer coefficient between the absorber and the heat transfer medium air, resulting in a significantly reduced collector efficiency factor (F') for air heating collectors. As a consequence, the temperature difference between absorber (T_{abs}) and the mean temperature of the heat transfer medium (T_m) is much higher for air heating than for liquid heating collectors. A lower efficiency factor (F') also leads also to higher values for the collector parameters (a_1 , a_2), because for the same mean operating temperature of the medium (T_m) the absorber temperature (T_{abs}) will be higher corresponding to higher thermal losses.

For covered liquid collectors the collector parameter η_0 , a_1 , a_2 are considered constant regarding the mass flow (\dot{m}) of the heat transfer medium (liquid). Although this simplification is acceptable for liquid based collectors, it is not for air heating collectors. Therefore equation 1 is rewritten for covered air collectors as:

$$\eta_{covered\ air\ coll} (G, T_m, T_a, \dot{m}) = \eta_0(\dot{m}) - a_1(\dot{m}) \frac{T_m - T_a}{G} - a_2(\dot{m}) \frac{(T_m - T_a)^2}{G} \quad (\text{eq. 4})$$

Therefore, the performance curve of air heating collectors must state the mass flow used in the tests.

For a better understanding of the dependency of air heating collector efficiency on mass flow, simulations and measurements for covered air heating collectors have been carried out. A 1x2 m² flat plate air heating collector with under-finned and under-flown absorber (similar to B2 in Fig. 1) was mathematically modelled to investigate this issue and other physical phenomena. The 2 m long finned flow channel runs parallel to the length of the collector. One channel in the middle of the collector was divided into a number of equal length segments. Each segment was modelled by seven temperature nodes interacting with each other through heat exchange phenomena. After simulating the first segment at stationary conditions, its outlet air temperature was used as inlet temperature of the second segment, and so on until the last. Thermal effects at the collector edges were neglected.

In addition to the simulation, measurements on different covered solar air heating collectors were carried out at the TestLab Solar Thermal Systems of Fraunhofer ISE, after the test stand was improved in order to achieve similar accuracy in temperature measurements and mass and heat flow as for measurements on liquid heating collectors.

The collector performance curve was simulated for different mass flow rates with the model described. Figure 4 shows the dependence of the collector performance curve on the mass flow. The curves for the laminar flow range (mass flow $m_{pkt} = 60 \text{ kg h}^{-1}$, blue graph), for the transition zone ($m_{pkt} = 200 \text{ kg h}^{-1}$, red graph) and for the turbulent range ($m_{pkt} = 600 \text{ kg h}^{-1}$, green graph) are presented. Since a 2 m² collector is simulated, the mass flow corresponds to 30, 100 and 300 kg h⁻¹ m⁻².

As expected, the efficiency increases with increasing mass flow (\dot{m}), since the heat transfer from the absorber to the heat transfer air improves with increasing mass flow. The lower the mass flow, the more the absorber temperature (T_{abs}) remains above the mean air temperature (T_m), due to the lower heat transfer coefficient. But with a higher absorber temperature (T_{abs}) the heat losses are higher and therefore the efficiency is lower.

Fig. 4 shows that the performance curves of an air heating collector strongly depend on the air mass flow rate. It is recommended that measurements of air heating collector performance be conducted using three different mass flow values.

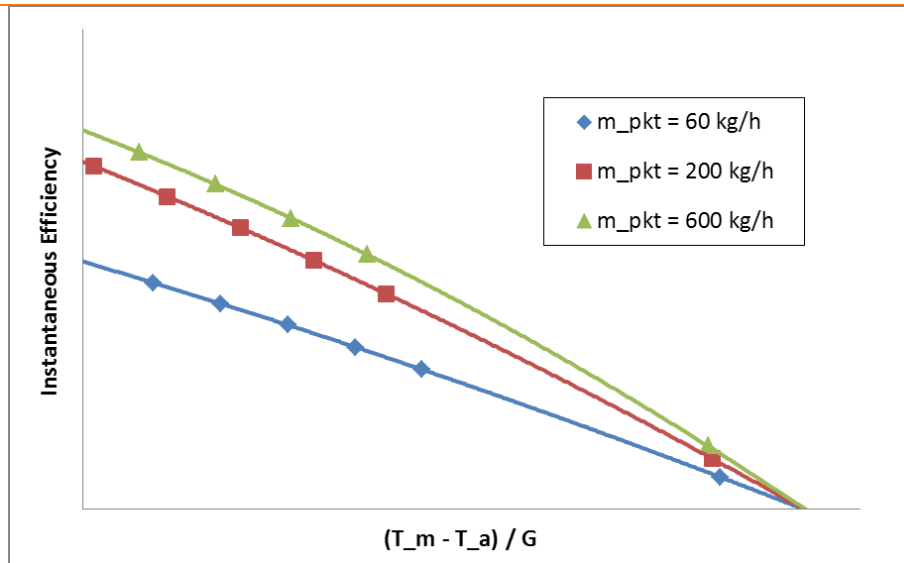


Fig. 4: Simulated performance curves of a 2 m² flat air heating collector for three mass flow rates (60, 200 and 600 kg h⁻¹)

Fig. 5 shows from measured data how the collector outlet temperature ($T_{\text{air}}(\text{out})$) and the absorber temperature ($T_{\text{abs}}(\text{out})$) near the outlet depend on the air mass flow rate (\dot{m}). In addition, the dependency of the useful thermal power ($Q_{\text{flow}}(\text{out})$) on the air mass flow is shown. The measurements were taken with a nearly constant inlet temperature ($T_{\text{air}}(\text{in})$) and a constant irradiation (G) of 993 W/m^2 . Both the absorber and air temperatures decrease with increasing mass flow (\dot{m}); the difference increases up to a mass flow rate of about 350 kg/h and then decreases (not shown in a separate line). However, the difference between $T_{\text{abs}}(\text{out})$ and $T_{\text{air}}(\text{mean})$, shown in figure 4 as well, decreases continuously.

The following phenomena influence the difference between the absorber and the air temperature at the collector outlet. With increasing mass flow:

- the heat transfer between absorber and medium air improves and therefore the temperature difference decreases;
- the residence time of the air within the collector decreases;
- the useful thermal power removed increases, thus the overall thermal losses decrease.

With other things being equal, the useful thermal power (\dot{Q}_{out}) is proportional to the mass flow (\dot{m}), due to:

$$\dot{Q}_{\text{out}} = \dot{m}c(T_{\text{out}} - T_{\text{in}}) \quad (\text{eq. 5}),$$

where (c) is the heat capacity of the medium.

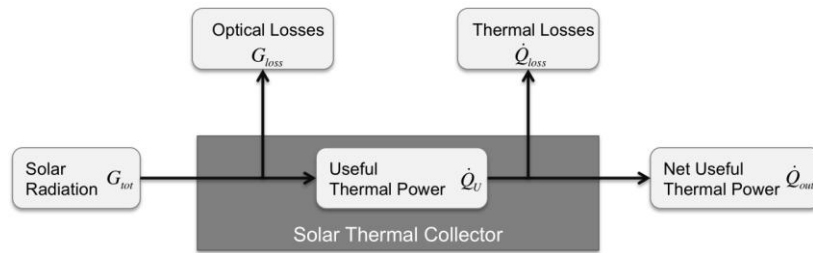


Fig. 5: Definition of the radiation and thermal energy flow through a solar thermal collector

At low mass flow rates the useful thermal power which can be removed is low. The principal energy flow through a collector is shown in Figure 5. When exposed to solar radiation, the absorber temperature rises to the point, where the sum of the thermal losses (\dot{Q}_{loss}) and the net useful thermal power (\dot{Q}_{out}) is equal to the irradiation (G_{tot}) minus the optical radiation losses (G_{loss}), since the thermal losses mainly depend on the temperature difference between the absorber and the ambient:

$$G_{tot} = G_{loss} + \dot{Q}_{loss} + \dot{Q}_{out} \quad (\text{eq. 6}).$$

The net useful thermal power (\dot{Q}_{out}) dependence on the mass flow is shown in Fig. 6, named $Q_{flow}(out)$ and normalized to the lowest measured value at 40 kg/h (right axis). Since the irradiation does not vary the net useful thermal power is equal to the efficiency and is thus increasing within the mass flow range shown.

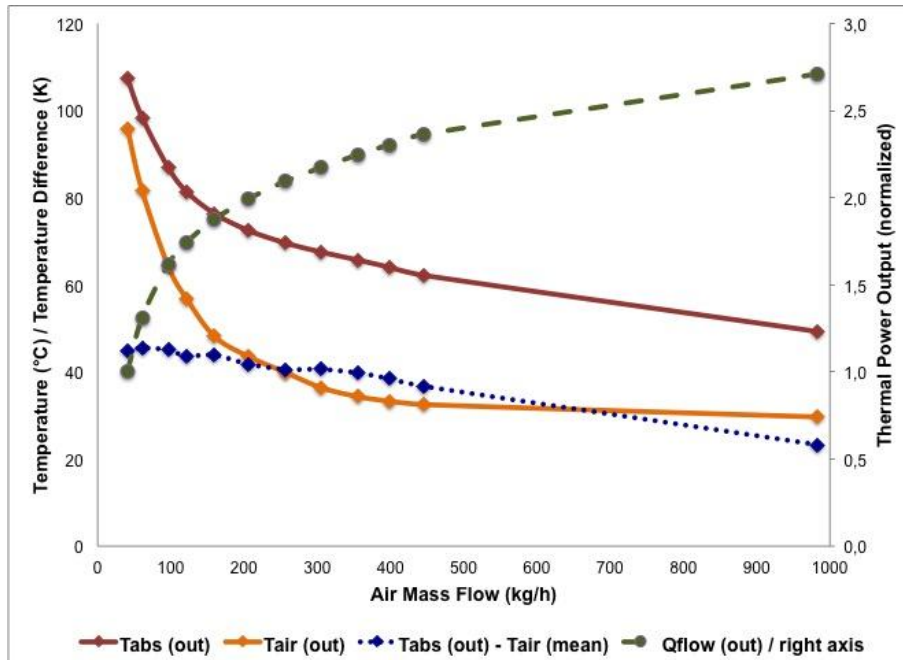


Fig. 6: Measured temperatures of absorber and air at the outlet of the collector, difference between absorber temperature at the outlet and the air mean temperature as well as the net useful thermal power (normalized, right axis) and their dependency on the mass flow

Figure 5 indicates that with increasing air mass flow the efficiency of the collector increases towards an asymptote while the temperature difference between the absorber and the mean temperature of the heat transfer air is continuously decreasing. While it appears that the highest possible air mass flow rates will achieve the greatest efficiency, the increasing electricity demand for the ventilator must be taken into account and an operational optimum found.

At low mass flow rates between 40 and 200 kg/h the temperature and power curves are very sensitive to the mass flow rate. This range corresponds with specific mass flow rates between 20 and 100 kg/h/m²; the air mass flow in commercially available air heating systems is typically in the range of 60 to 150 kg/h.m² according to the manufacturer's specifications. Thus the influence of the mass flow rate must be considered carefully for air heating collectors.

The collector efficiency factor (F') was determined by simulations for various mass flow rates in order to determine its influence. Figure 7 shows a very strong efficiency increase for mass flow rates up to 200 kg/h (100kg/h/m²), demonstrating the high sensitivity of efficiency to mass flow in this range.

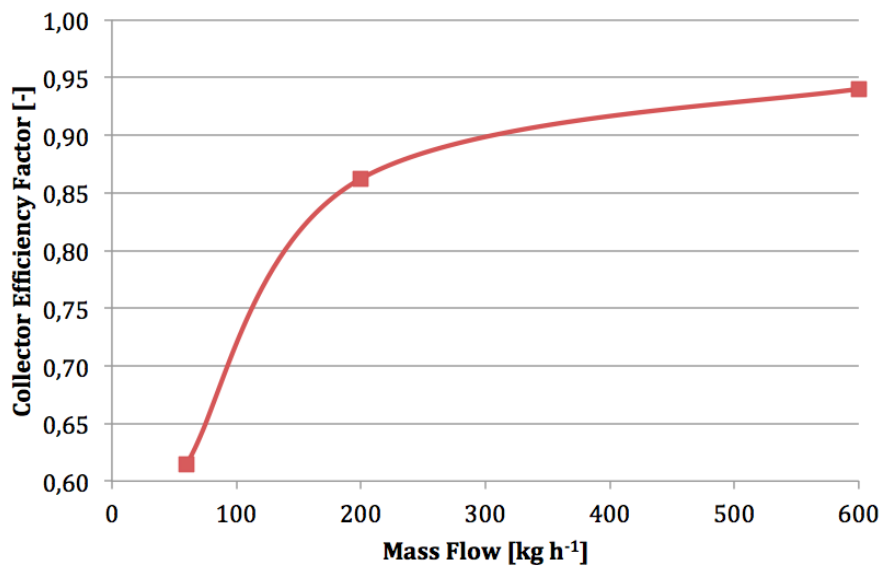


Fig. 7: Simulated dependency of the collector efficiency factor (F') on the mass flow

The collector efficiency factor (F') reflects the heat transfer coefficient between the absorber and the heat transfer medium in the maximum thermal efficiency ($\eta_0(\dot{m})$) in equation 4, but it also occurs in the heat losses factors ($a_1(\dot{m})$, $a_2(\dot{m})$). In the first case the collector efficiency factor increases with increasing mass flow by increasing the heat transfer coefficient between absorber and heat medium, in the second case it increases due to the decreasing absorber temperature and therefore lower losses for a given temperature difference ($T_m - T_a$).

Since at the collector stagnation point the mass flow is zero per definition, and thus the net useful thermal power (\dot{Q}_{out}) is zero. The full power of incoming radiation resulting in a useful thermal power is then dissipated through thermal losses. The losses are mass flow independent because mass flow is zero at this point. When efficiency curves for different mass flow rates are extrapolated they thus all pass through the same stagnation point.

4.3 Reference temperature for the performance curve

To generate a collector efficiency curve it is important to define in the standard the reference temperature for which the performance curve is presented, i.e. the temperature used on the x-axis besides the ambient temperature. For liquid heating collectors the reference temperature is the mean temperature (T_m) of the liquid as described in equation 1. For air collectors two different solutions are in use. The American ANSI-ASHRAE 93 and the Canadian CSA F378.2 standards use the inlet air temperature (T_{in}) as the reference temperature. In contrary, the IEA-Task 19 recommends the outlet air temperature (T_{out}) as the reference temperature for generating a performance curve. The reasons for these different approaches include the following.

In North America mainly non-covered open to ambient air heating collectors are used. Therefore the inlet air temperature is equal to the ambient temperature and the temperature increase in the collector is rather small. When the inlet air temperature is used as the reference temperature, the measurement process is simplified. IEA Task 19 presumably focused more on covered air heating collectors and took into account the large temperature difference between the absorber and the air heat transfer medium. Since the temperature profile of the air flowing through the collector is not exactly known, the outlet air temperature is closer to the absorber temperature than the mean air temperature, and the temperature difference between the absorber and ambient is the relevant parameter for calculating the thermal losses, the outlet temperature was recommended.

There are four considerations (aspects) which should be taken into account when deciding which reference temperature to use:

1. How is the measurement of the performance curve influenced by the reference temperature?
2. How will the performance curve be used for comparison between solar thermal collectors?
3. How does the reference temperature influence the quality of the performance curve?
4. How will the performance curve be used for simulations of solar air heating systems?

Regarding aspect 1: When an open to ambient collector is measured, the inlet air temperature is equal to the ambient temperature. Since the mean and the outlet temperatures are fixed for a given radiation and mass flow, it does not matter which temperature is chosen as reference. However, open to ambient collectors have only one efficiency value for a given mass flow and irradiation, and different manufacturers may specify different mass flows per m^2 . The same reference temperature value must be used for all collectors. It requires more effort to perform the measurement for the same mean or outlet temperature for all collectors, because the mean and the outlet temperature depend on the efficiency of the collector. Therefore, while it is much simpler to reference the performance of open to ambient collectors using the inlet air temperature, it is also possible to use the mean or the outlet temperature.

In the case of closed loop collectors an efficiency curve can be generated by varying the inlet temperature. Therefore no restrictions apply here to which reference temperature can be used.

Regarding aspect 2: The main reason to unify collector performance standards is to allow for comparison of performance independent of the collector construction or heat transfer medium. In most cases concerning liquid heating collectors the mean temperature of the fluid is used as the reference temperature, so a direct comparison via mean temperature of the air as the reference temperature for air heating collector performance is possible.

Regarding aspect 3: The thermal losses of a collector depend mainly on the mean temperature of the absorber. The performance of a solar collector, according to equation 1 and 4, depends on the temperature difference between T_m and the ambient temperature T_a . To determine the mean temperature, the inlet and the outlet temperature need to be measured. For the same mean temperature many inlet temperatures are possible, by adjusting the mass flow rate to achieve the desired outlet temperature. The same applies for the outlet temperature. This means that if either the inlet or the outlet temperature alone were to be used as the reference temperature without defining the other temperatures, the result would not be sufficiently defined.

Regarding aspect 4: Simulation models calculate the outlet temperature of the collector for a given inlet temperature using the efficiency of the collector. If only the inlet temperature were used as the reference temperature, the efficiency would be independent from the temperature difference between inlet and outlet temperature, which is physically not possible. This is the same argument as in aspect 3.

Therefore, only the mean temperature can be used as reference temperature for well-defined measurements of the performance curve. For this reason the mean temperature is proposed as the reference temperature for air heating collectors in the draft for EN 12975. Where the difference between inlet and outlet temperature is limited and the measurement conditions are fairly constant, as is the case when measuring non-covered, open to ambient

collectors, the inlet temperature could be used by proxy.

Therefore, the question is: how can the mean temperature can be determined. The temperature difference between the absorber and the heat transfer air is usually large, and an asymptotic profile for both from the results of the aforementioned simulations of air and absorber temperatures along the collector channel, shown in figure 8. The heat transfer coefficient for each segment is also shown. The temperature increase of the air in the collector is nearly linear from the inlet to the outlet except for the ‘run-in’. This result was also validated by measurements. It was therefore determined that the mean temperature can be calculated in the same way for air heating collectors as for liquid heating collectors, i.e. as the arithmetic average of inlet and outlet temperature as described in equation 3.

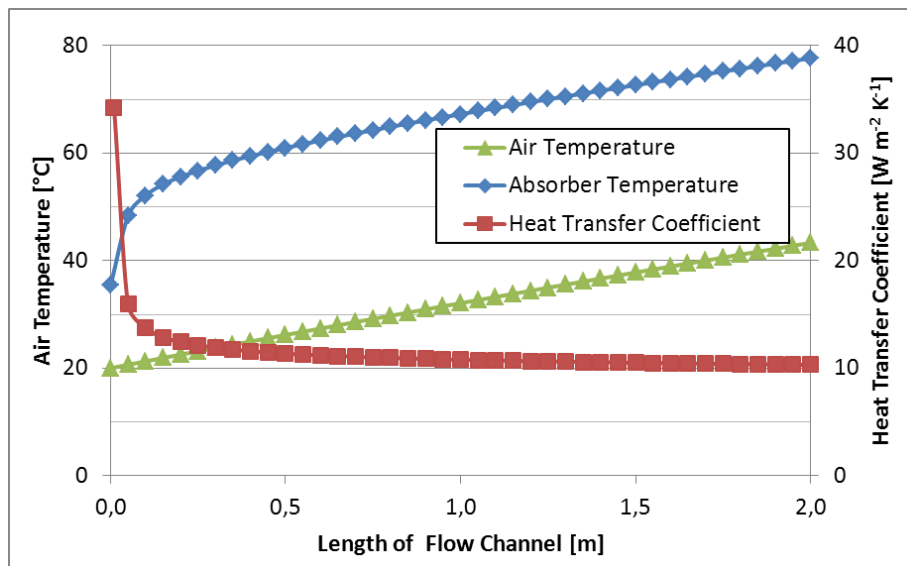


Fig. 8: Simulated temperature of the heat transfer air and the absorber as well as the heat transfer coefficient

4.4 Detailed work on measurement methods and leakage rate to achieve suitable accuracy

The temperature of the air in a channel depends on different variables; therefore a comprehensive analysis using computational fluid dynamics is needed to simulate the behavior. The equations describing the situation are the continuity equation (7), the moment equation (8) and the energy equation (9). These equations in differential form are:

$$\frac{\partial \rho}{\partial t} + \nabla \cdot (\rho v) = 0 \quad (\text{Eq. 7})$$

$$\rho \frac{dv}{dt} = \rho g - \nabla p + \nabla \cdot \tau_{ij} \quad (\text{Eq. 8})$$

$$\rho \frac{de}{dt} + v \cdot \nabla p = \nabla \cdot (k \nabla T) + \nabla \cdot (v \cdot \tau_{ij}) \quad (\text{Eq. 9})$$

ρ - density
 t - time
 v - velocity
 g - gravity of earth
 p - pressure
 τ - friction term
 k - thermal conductivity
 e - specific energy
 u - specific internal energy
 T - Temperature
 c - specific heat
 A - area

According to these equations there are five variables (ρ , V , p , u and T), however only three equations are provided. The other two necessary equations are for the state of a gas.

$$\begin{aligned} \rho &= \rho(p, T) \\ u &= u(p, T) \end{aligned} \quad (\text{Eq. 10 and 11})$$

Theoretical solutions for these problems can only be provided by making many assumptions, such as that the fluid to be modeled is behaving as a Newtonian fluid, or that the fluid is either incompressible or an ideal gas. Computational fluid dynamic programs are often applied to solve more complicated (and closer to reality) situations.

The calculation of the temperature in air channels involves many variants and must be analyzed carefully. One example is that due to the air density gradient induced by temperature differences and changes in the floating directions, flowing air in a circular pipe cannot be considered to be axial symmetric.

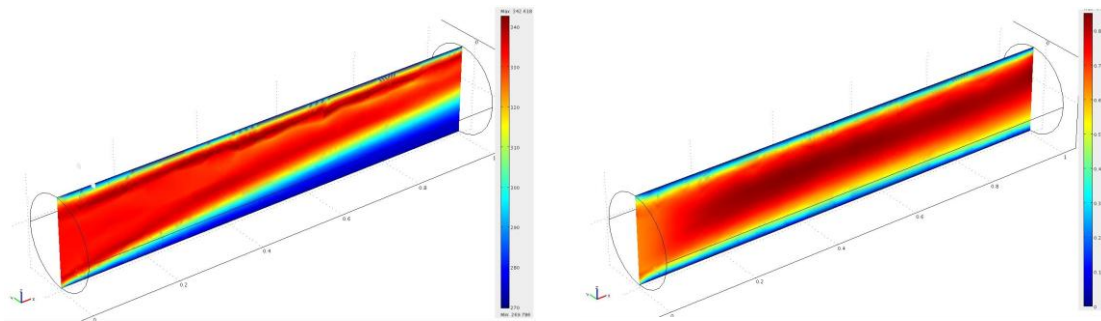


Figure 9 and 10: Results of fluid dynamic analysis of the temperature distribution (left) and the air velocity distribution (right) of an air duct of one meter length. The flow direction is from left to right. The minimum values (blue) are 0°C (273 K) and 0m/s; maximum values (red) are 67°C (340 K) and 0.85 m/s. ©Fraunhofer ISE

In order to describe the temperature of devices like solar air heaters which are assembled from different parts and materials it is reasonable to define a thermal mean temperature; in this case this mean temperature is defined as the sum of all single parts weight with their respective heat capacity and temperature in relation to the sum of their thermal capacity and mass.

$$T_{m,th} = \frac{\sum_{i=1}^n m_i c_i T_i}{\sum_{i=1}^n m_i c_i} \quad (\text{Eq. 12})$$

This equation has to be transformed to describe the real mean temperature in the air channel. Therefore an integral over the entire normal surface area needs to be determined considering all the depending variables. With this transformation the thermal mean temperature is called mixed-temperature.

$$T_{m,th} = \frac{\int T(A) v(A) \rho(A) c(A) dA}{\int v(A) \rho(A) c(A) dA} \quad (\text{Eq. 13})$$

Deriving from this equation one can see what parameters have to be measured at each point of the cross section area to find a mean temperature of the testing fluid. These are:

- local temperature
- local density
- local heat capacity (depending on humidity)
- local air velocity

Equation (14) shows that the temperature is beneath others depending on the fluid velocity. This means that the temperature measurement must consider the velocity profile in order to arrive at an accurate result. To simplify the process one can consider the density and the specific heat as constant within one cross section area along the channel [1].

The reduced expression for the mixed temperature is then as follows:

$$T_{m,th} = \frac{1}{Av_m} \int T(A)v(A)dA \quad (\text{Eq. 14})$$

4.5 Comparison of two methods for temperature measurement in gas streams

In the following sections two methods for temperature measurements are described, their advantages and disadvantages are discussed, and a suggestion is made about how the measurement can be standardized. The aim is to identify a suitable method to measure the reference temperatures for a caloric characterization of solar air heaters.

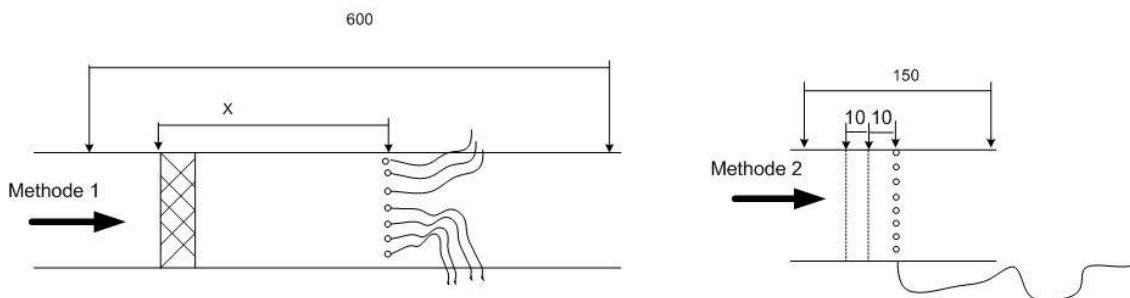


Figure 11: Sketch of method 1 using a blender and multi-sensor temperature measurement unit (left) and method 2 using two net and an integrating temperature sensor (right)

4.5.1 Method 1: Multi-temperature sensors with air blender

In this method the gas is mixed with an air blender (Figure 11 left) to ensure a preferably homogenous temperature profile. This profile is homogenous but only at a certain distance behind the blender depending on the Reynolds number of the flow situation.

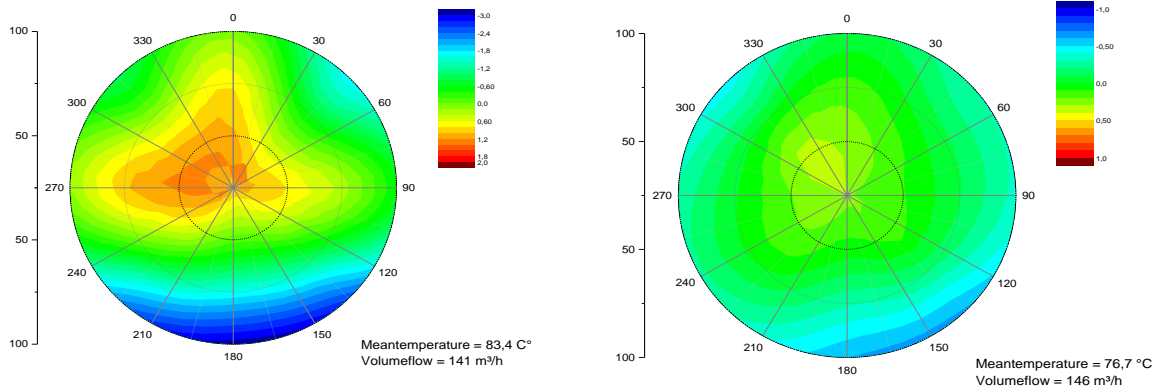


Figure 12 (left) and 13 (right): Temperature distribution measured in a 200 mm air duct. The left figure shows the temperature distribution without blender. The mean temperature is 83.4 °C, the temperature variation is 3.3 K; the volumetric flow is 141 m³/h. The right figure shows the mixed air temperature by using an air blender measured 34 cm behind the air blender. The mean temperature is 76.7 °C, the temperature variation is 0.7 K; the volumetric flow is 146 m³/h. ©Fraunhofer ISE

By using an air blender the homogeneity of the temperature distribution across the surface at a certain distance after the blender can reach values up to +/- 0.35 K. In this case, when an air blender was not used the temperature differences exceeded 3.3 K. The distance between blender and temperature measurement influences the homogeneity as well as the velocity of the air stream. These influences are shown in figure 6.

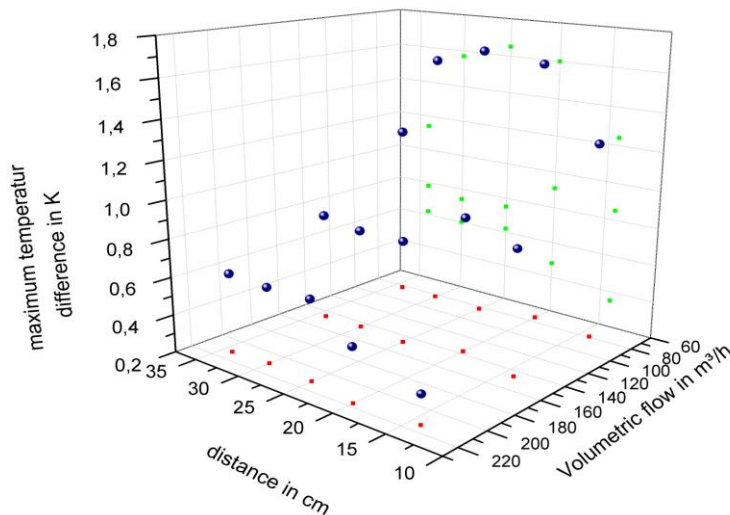


Figure 14: Maximum temperature differences within a cross section caused by the distance between blender and temperature sensor unit and by the velocity (volumetric flow) of the stream. The green and red points are the projected measured points in xy-plane and yz-plane. ©Fraunhofer ISE

The distance between temperature sensor and air blender was varied from 140 to 350 mm for these experiments. The complete length of the temperature measuring device including the air

blender exceeds 600 mm, and the entire length must be properly insulated in order to achieve accurate temperature measurements.

Table 4: Advantages and disadvantages of method 1

Advantages	Disadvantages
Repeatable and accurate temperature profile achieved by installing a blender	Dependence of the distance between air blender and temperature sensor on the Reynolds number. The temperature sensor has to be moved depending on air velocity. In normal operation the sensors are fixed at one position with the result of higher inhomogeneity.
The blender generates only low pressure losses in the measurement channel	The measurement error depends on the homogeneity of the temperature distribution
	Large surface area of the air channels leads to thermal losses because the channel length is determined by operational considerations described above
	Thermal losses must be considered in the thermal performance of the solar air heater. Due to the high number of sensors needed it is not possible to calibrate the thermal losses of the sensors
	Many sensors are needed in order to provide a good homogeneity

4.5.2 Method 2 – integrating temperature sensor with two nets

In method 2 the sensor unit consists of two nets along the channel within a distance of 10 mm in order to provide a uniform velocity profile (see figure 11, right). The temperature is measured behind these nets with a spiral sensor homogeneously covering the channel area [3]. The distance between the net and the spiral sensor is 10 mm.

The length of the equidistant temperature sensor depends on the diameter of the air duct and the radial distance between each winding of the sensor. The geometry of the nets has to be analyzed in case studies, as it depends on the volumetric flow and the diameter of the air duct.

Table 5: Advantages and disadvantages of method 2

Advantages	Disadvantages
Velocity profile can be considered uniform	Need to analyze the effect of the net on air flow. An optimized net is required for this measuring method.
Only one signal sensor	Pressure drop caused by the sensor
Smaller space needed leading to a smaller surface area. The distance between temperature sensor and solar air heater can be reduced to 100 mm. The total construction length can be reduced to 150 mm	

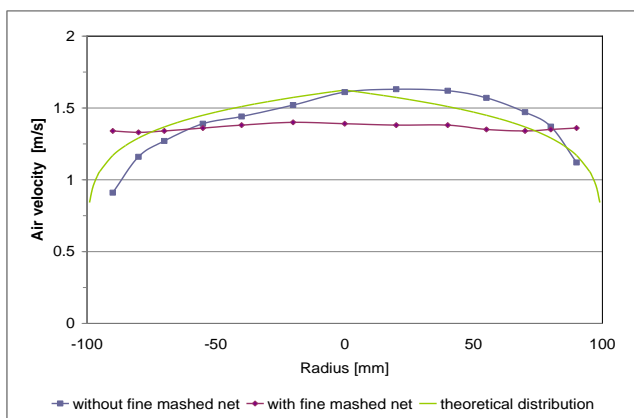
Preconditions for using method 2 are a homogenous velocity distribution and a requirement that the nets have no influence on the temperature measurement. Three case studies representing different configurations help model a properly working temperature sensor. The reason for developing these three different studies is to provide different flow conditions and study the effect on the temperature profile and consequently the effect on the temperature measurement. These situations are assumed to occur when characterizing different air heater products.

The first configuration consists of a 3 m straight pipe where the sensor is placed at the end of the pipe.

In the second configuration the sensor is placed behind a 90° elbow. In front of the elbow a 3 m pipe is placed in order to avoid disturbance on the fluid profile.

The third case study is a diffuser causing a diameter change from 120 mm to 200 mm.

Effect of the net on flow speed

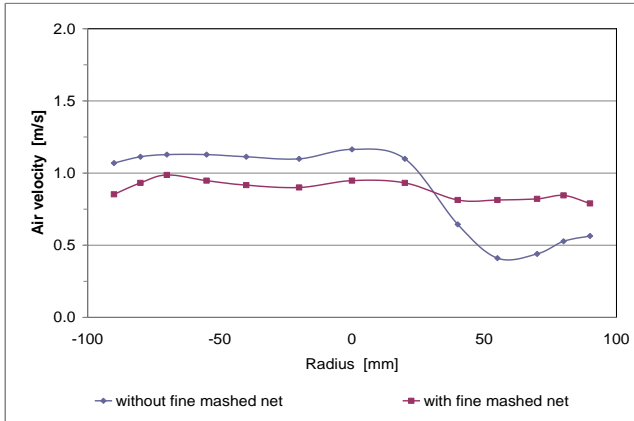


In figure 15 the distribution of the air velocity in a horizontal line through a straight air duct is shown (flow direction from bottom to top). The blue line shows the measurement values without fine meshed nets. The violet line shows the straightened profile after the fine meshed nets. The green line demonstrates the theoretical line calculated according to NICURADSE. The calculated variance is

reduced significantly by using the fine meshed net (from $5 \cdot 10^{-2}$ to $5 \cdot 10^{-5}$).

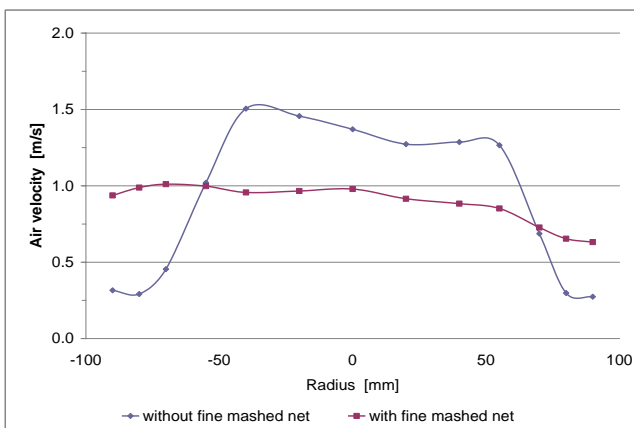
Figure 15: Distribution of the air velocity in a straight air duct

Figure 16: Distribution of the air velocity after a 90° elbow



The blue line in Figure 16 shows the velocity profile after a 90° elbow. The inner circular part of the elbow (positive radial values) shows a reduced velocity. The outer circular part of the elbow shows a higher velocity. Both effects are compensated by the net. Variance is reduced from $9 \cdot 10^{-2}$ to $4 \cdot 10^{-3}$ by using the nets.

Figure 17: Distribution of the air velocity after a diffuser 120/200 mm



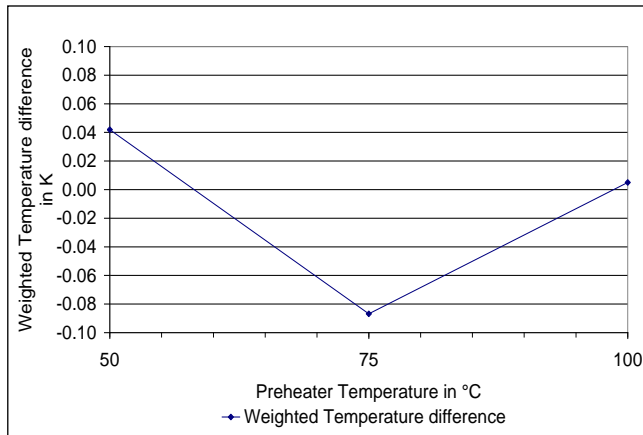
The air ducts in solar air heaters often vary in the geometry and it is necessary to use diffusers in order to adapt them to measurement devices. In this case the distribution of air velocity is extremely disturbed. In figure 10 this distribution is represented by the blue line. The effect of diameter change from 120 to 200 mm is reflected in the flow distribution. The fine meshed net reduced the inhomogeneous profile. The calculated

variance is reduced from 0.253 to 0.017 by using fine meshed nets.

It can be observed that the net provides a uniform velocity profile. Therefore the temperature measured by the spiral sensor is accurate since there is not need to weight the temperatures across the cross section.

4.5.3 Effect of fine mesh nets on temperature

To analyze the influence of the net on temperature the following experiment was performed. The air stream was heated, after temperature and volumetric flow were measured with and without net. In order to estimate possible effects of the net on the temperature in stationary conditions, such as heat transfer or radiation exchange from the net to the channel surface or to the sensor surface, the volumetric flow was kept constant. The temperature was measured in a horizontal axis with 6 points covering the same circular area. The temperature was weighted by the velocity. Figure 18 shows the difference of this weighted temperature and the temperature of the air heater.



These results show that the net has no significant effect on the measured temperature and its influence can be neglected in a stationary measurement.

Figure 18: Weighted temperature difference at different preheated temperature levels (50, 75 and 100 °C)

4.6 Conclusions regarding measurement of air flow and temperature

Both methods of measuring temperatures in air channels lead to accurate results if they are executed in the proper way. Both types of sensor units have advantages and disadvantages. When using the temperature sensor with an air blender (method 1) many single point sensors are needed. The minimum number of sensors should be 12 per temperature measurement point for a 200 mm air duct. This leads to a relative high uncertainty regarding the calibration of the sensor units.

Because of the fact that the homogeneity of the temperature depends on the temperature level, the geometry of the air duct and also on the flow parameters, the measured arithmetic mean temperature differs from the real mean weighted temperature (Equation 13). To reduce the error of measurements different temperature layers have to be mixed to produce an acceptable mean value. The ANSI ASHRAE 93:2003 requires a value with a tolerance of ± 0.5 K [2]. To reach this value a properly working air blender is required.

The temperature profile uniformity when using a mixing device depends on the Reynolds number of the flow and the distance between the air blender and temperature sensors. To accurately characterize a solar air heater it must be measured with several volume flows, therefore the temperature homogeneity can vary. The advantage of this sensor configuration is that temperature profiles can be visualized. On the other hand the complete construction length can exceed 600 mm. The heat losses over the channel lengths before and after the solar air heater have to be considered when calculating the solar air heater performance. Therefore this method is very sensitive to varying products and boundary conditions and seems to be difficult to use.

In the case of using the temperature sensor with nets (method 2), only one sensor is needed. The sensor is configured to uniformly represent the cross section of the air duct. This can be accomplished by configuring the sensor in an Archimedean spiral. To be able to use Equation 14 and ensure that the measured temperature is the mean weighted temperature the air

velocity has to be uniform. This can be accomplished by placing two fine mesh nets short distances in front of the temperature sensor. The fine mesh nets guarantee that the distribution of the air velocity is homogenous even after the air has passed through a 90° elbow or a diffuser. With additional case studies optimized mesh net geometry can be found. The length of this kind of sensor can be reduced by up to 3/4 in comparison with the length of the sensor unit using an air blender. The sensor measures the temperature directly at the solar air heater inlet and outlet. Due to this fact the influence of the surrounding environment is reduced (the influence of heat losses, wind speed and irradiation). The heat loss between inlet and outlet sensor can be calibrated in such a way that no recalculation is necessary.

Therefore we suggest the application of method 2 with a spiral temperature sensor and net assembly as the standardized method for temperature measurements in air ducts for the characterization of solar air heaters.

4.7 Performance test methods for uncovered/covered, open to ambient and closed loop collectors

As described above test sequences for air heating and water heating collectors have many common features, however significant difference between open to ambient air collectors and covered, or glazed collectors must be made. Open to ambient collectors always use ambient air as inlet air and heat this air flux to the outlet air temperature. This makes the boundary conditions for η_0 measurements difficult to control and prepare. Since air heating collectors may have a significant ΔT over the collector, to have a mean value of t_m on the same temperature level as t_{amb} , makes low inlet temperatures necessary. For example, if the collector efficiency is high, the inlet air temperature at near η_0 conditions may be raised by 40°K at the outlet. To raise t_m to the level of t_{amb} , inlet air at a temperature of around 0°C would be required. However, heating the air in the collector will change its capacity for humidity significantly. So this would lead to conditioned air for the measurement which is not realistic anymore. In addition to this effect, the inlet temperature for open to ambient collectors is the ambient temperature, however if cold inlet temperature air is provided as just described, the t_m would again not be at t_{amb} . These effects lead to the conclusion that specific temperature operating points and the respective efficiencies and power outputs should be generated, rather than curves to extrapolate.

A similar effect happens when describing the IAM of open to ambient collectors. The IAM should describe only the optical losses from a varying incidence angles. To measure these influences empirically the boundary conditions when the mean heat losses of the collector are zero under perpendicular radiation are determined, and then determined again for each of the different incidence angles required. As noted previously the η_0 conditions are not possible to provide in some cases. As a consequence, the IAM may not be able to be determined empirically if the no-thermal-loss conditions are not provided. This effect is especially true for collectors where the mass flow is directly controlled by an integrated PV module. In such a collector, the fan generating the mass flow and therefore determining the operation point is

provided with electricity from an integrated PV module. The result is that the higher the irradiance, the higher the mass flow, the more heat exchange, and thus the more heat power output. Calculating a yearly energy output on the basis of standard collector parameters is complicated for this type of product. The mass flow dependency of the thermal collector performance is linked to the angle dependency of the PV module, in turn resulting in an IAM for thermal performance.

The effect of wind on the thermal convection losses of a collector is an important parameter for all collector types. For an evacuated tube collector (ETC) the external convective losses are significantly reduced by the vacuum. For a standard flat plate collector (FPC) with a transparent cover and some gap between the absorber and the cover optimized to have no internal convection transporting significant heat from the absorber to the front cover, the wind dependency can be measured but has often proven to be in a low range. Wind effects may be more pronounced on collectors where the front cover is either in direct contact with the heat transfer medium, or collector designs without any protection against convection losses (such as unglazed), and these effects must be quantified. The values from the measurements can then be used for calculations and simulations. The dependency is described by Equation 15:

$$\frac{\dot{Q}_m}{A \cdot G''} = \eta_{\max,0m/s} - b_u \cdot u \tag{Eq. 15}$$

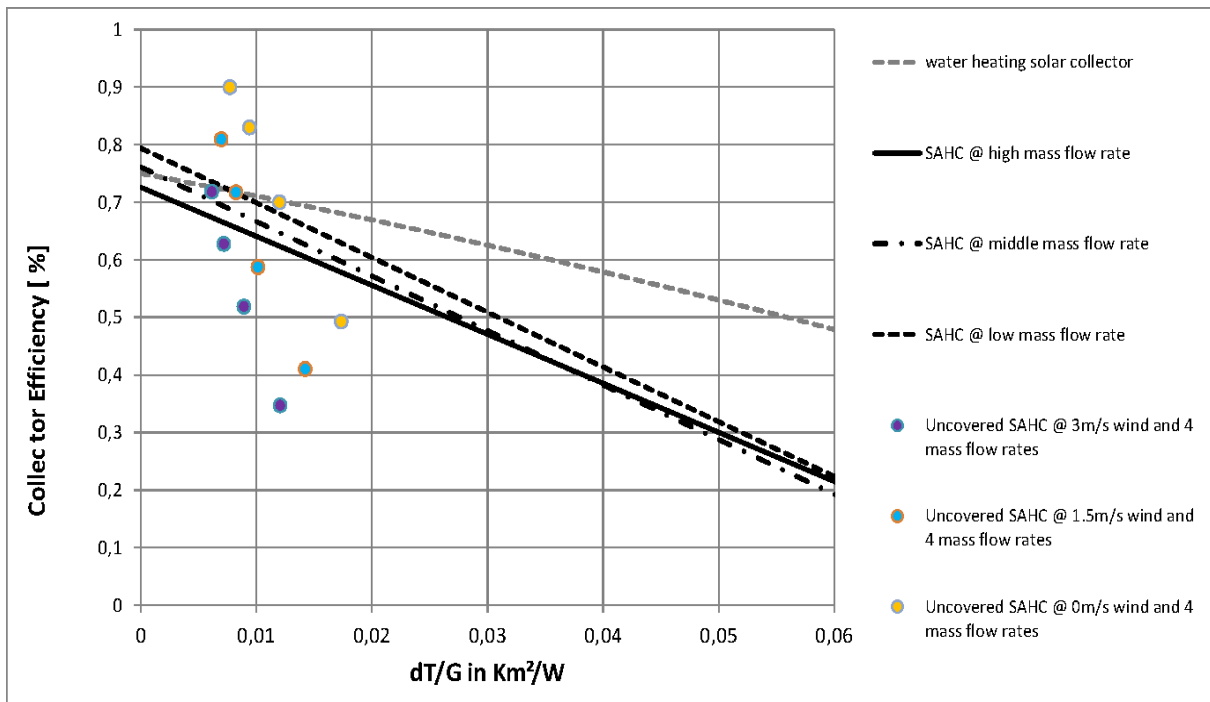


Figure 19; the graphic shows dependencies of collector performance on dt/G, mass flow rates and wind speed

4.8 Simulation tools for different technologies and applications

To calculate economic performance and convince a potential customer to purchase a solar air heating system, it is necessary to simulate the solar yield of a solar air heating system at a specific site and under the specific conditions. For solar liquid heating collectors several well-known and validated simulation programs are available. For air heating systems two commercial tools are available, however they are unable to simulate some of the commercially available solar air collectors on the market.

The free program ‘RETscreen’ is made available by the Ministry of Natural Resources Canada (NRCan) (RETscreen, 2011). The spreadsheet-based program calculates system yields for non-covered (unglazed) transpired air collectors. A selection can be made between ventilation air heating and process air heating. The results include values for life-cycle costs, greenhouse gas emission reductions and product energy production.

The second program ‘TSol’ (Pro Version 5) is available from Dr. Valentin EnergieSoftware GmbH and can calculate two system configurations (Valentin, 2011). One is for domestic air heating, the other for domestic air heating in combination with solar domestic water heating. TSol provides a choice between fresh air (‘open’) and recirculating (‘closed’ loop) system configurations. The results include system efficiency, greenhouse gas emission reductions and savings of natural gas.

In order to predict the energy production of a solar air heating system in detail and optimize the technology and the design of solar air collector systems, a more detailed simulation tool verified with reliable test data of the solar air collectors is necessary. Fraunhofer ISE is developing a solar air collector Type for the simulation tool TRNSYS in order to model different solar air heating collectors and systems. A yield calculation is also important because it is required for accessing subsidies for solar thermal collectors in Germany.

5 AIR COLLECTOR TESTS

Figure 19 (above) shows efficiency test results for different solar air heating collectors. Tests for performance and functional tests for methodology validation have been carried out. The tests on function provide important information, and in some cases may be the reason for not meeting the requirements of the Solar Keymark label. In the experience of Fraunhofer ISE, the collectors ability to withstand mechanical loads induced by wind and snow and the tendency to accumulate high levels of condensation inside collectors are the two most common factors for failing performance and durability tests.

6 ANNEX: SUBTASK A ROADMAP CONTENT RELATED TO AIR HEATING COLLECTORS

The Subtask A Roadmap content was developed for this section, and appears as part of the Roadmap of Collector Testing and Certification Issues (Subtask A.1).

7 REFERENCES

- [1] Stryi-Hipp, G., Kramer K., Richter J., Thoma Ch.,Fortuin S., Mehnert S. and Welz Ch.; *TOWARDS A UNIFIED STANDARD FOR SOLAR AIR HEATING COLLECTORS* , ISES SWC 2011, Kassel, Germany
- [2] F. Brenhard (2004): *Technische Temperaturmessung* , Springer Verlag
- [3] ANSI ASHRAE 93 - 2003: *Methods of Testing to Determine the Thermal Performance of Solar Collectors*
- [4] R. Digel: *Messung der mittleren Temperatur strömender Luft in Kanälen unterschiedlichen Querschnitt.* Stuttgart, direkte Korrespondenz
- [5] Stryi-Hipp, G., 2010. Neue Perspektiven für Luftkollektorsysteme. Solarthermie-Symposium, May 2010, Bad Staffelstein, Germany
- [6] Thoma, C., Kramer, K., Cerezo, J. D., 2010. Temperature Measurements in Air Ducts – An Optimized Method for Solar Air Heaters, Eurosun, Graz.
- [7] ANSI/ASHRAE, 1993.American Society of Heating, Refrigerating and Air-Conditioning Engineers, 1991, ANSI/ASHRAE 93-1986 (RA 91): *Methods of Testing to Determine the Thermal Performance of Solar Collectors*, USA
- [8] IEA Task 19, 1999. Arsenal Research, Department of Renewable Energy, Hubert Fechner, October 1999, Solar Air Systems – Investigations on Series Produced Solar Air Collectors, Austria
- [9] Schüle, K., Siems, T., 2009. Vakuumröhren-Luftkollektor für hohe solare Deckungsgrade, published in: Erneuerbare Energie 2009-01, AEE Intec, Austria
- [10] RETScreen, 2011. RETScreen Clean Energy Project Analysis Software, www.retscreen.net
- [11] Valentin, 2011. T*Sol pro, The Dynamic Simulation Program for the Design and Optimization of Solar Thermal Systems, Valentin Software Inc., <http://valentin-software.com/xcartgold/T-SOL-Professional.html>
- [12] Fechner, H. (1999). IEA TASK 19 Solar air systems - Investigation on Series Produced Solar Air Collectors - Final Report. Vienna, arsenal research - Department of Renewable Energy.
- [13] Weiss, W., I. Bergmann, et al. (2009). Solar heat worldwide - Markets and contribution to the energy supply 2007. IEA Solar Heating & Cooling Programme. Gleisdorf, Austria, AEE - Institute for Sustainable Technologies: 48.
- [14] (2011). Luftkollektoren. Solarthemen: 6, 24.
- [15] Alvarez, G., J. Arce, et al. (2004). "Thermal performance of an air solar collector with an absorber plate made of recyclable aluminum cans." *Solar Energy* 77(1): 107-113.
- [16] Bambrook, S. and A. Sproul (2008). 084 - modelling the energy contributions of a PVT system to a low energy house in Sydney. EuroSun. Lisbon, Portugal.
- [17] Bodycote Testing Group (2008). Solar collector 1500 GS test report, Your Solar Home, Inc.
- [18] Brunger, A. P., A. Cali, et al. (1999). Low cost, high performance solar air-heating systems using perforated absorbers, IEA International Energy Agency.

- [19] Keller, J., V. Kyburz, et al. (1988). Untersuchungen an luftkollektoren zu heiz- und trocknungszwecken. Würenlingen, Schweiz, Paul Scherrer Institut.
- [20] Kraus, B. (2006). Abschlussbericht entwicklung und optimierung der einsatzmöglichkeiten einfacher solarer luftkollektoren aus bestehenden fassadenelementen im industriebau, Solar-Institut Jülich SIJ
- [21] Löffler, M. (2011). Verbesserung des wirkungsgrades von luftkollektoren durch grenzschichtabsaugung, simulationsergebnisse. Karlsruhe, Universität Karlsruhe.
- [22] Morhenne, J. (2002). Solare luftsysteme. BINE Informationsdienst themeninfo. Karlsruhe, Fachinformationszentrum Karlsruhe, Gesellschaft für wissenschaftlich-technische Information mbH: 12.
- [23] Morhenne, J. and B. Langensiepen (2005). Ertragsbestimmung und einsatzbereiche des makrosolar Kollektors bewertung mittels dynamischer gebäudesimulation, Ingenieurbüro Morhenne GbR.
- [24] Morson, I. (2007). Performance review of the SH 1500G solar air heater. Manufactured by Your Solar Home.
- [25] Perers, B., P. Kovacs, et al. (2006). Validation of a dynamic model for unglazed collectors including condensation. Application for standardised testing and simulation in Trnsys and Ida. EuroSun.
- [26] Renner, G. (2009). SolarLuft und wärmerückgewinnung, Grammer Solar.
- [27] Rid, U. (2011). Richtlinien zur förderung von maßnahmen zur nutzung erneuerbarer energien im wärmemarkt, Bundesministerium für Umwelt, Naturschutz und Reaktorsicherheit.
- [28] Romdhane, B. S. (2007). "The air solar collectors: comparative study, introduction of baffles to favor the heat transfer." Solar Energy 81(1): 139-149.
- [29] Shukla, A., D. N. Nkwetta, et al. (2012). "A state of art review on the performance of transpired solar collector." Renewable and Sustainable Energy Reviews 16(6): 3975-3985.
- [30] Stryi-Hipp, G., K. Kramer, et al. (2011). Towards a unified standard for solar air heating collectors, Fraunhofer Institute for Solar Energy Systems ISE, Freiburg
- [31] Thoma, C., J. D. M. Cerezo, et al. (2010). Temperature measurement in air ducts - an optimized method for solar air heaters. Eurosun. Graz, Austria.
- [32] Thoma, C., J. Richter, et al. (2011). Optimierung und validierung des luftkollektorteststandes im rahmen des projektes Luko-E.
- [33] Weaver, K. and C. Culp (2006). Static pressure losses in 6, 8, and 10-inch non-metallic flexible ducts. The International Conference for Enhanced Building Operations (ICEBO). Shenzhen, China.
- [34] A. A. Zomorodian, J. L. W. (2003). "Modeling and Testing a New Once-through Air Solar Energy Collector."
- [35] B.A. Fleck, R. M. M., M.D. Matovic (2001). "A field study of the wind effects on the performance of an unglazed transpired solar collector." 8.
- [36] Bambrook, S. and A. Sproul (2008). 084 - modelling the energy contributions of a PVT system to a low energy house in Sydney. EuroSun. Lisbon, Portugal.
- [37] Bodycote Testing Group (2008). Solar collector 1500 GS test report, Your Solar Home, Inc.
- [38] C. Dymond, C. K. (1996). "Development of a flow distribution and desing model for transpired solar collectors."
- [39] G. W. E. Van Decker, K. G. T. H., A. P. Brunger (2001). "Heat-exchange relations for unglazed transpired solar collectors with circular holes on a square or triangular pitch."

- [40] Hollick, J. C. (1999). "Commercial scale solar drying."
- [41] Hoy-Yen Chan, S. R., Jie Zhu (2011). "Experimental performance of unglazed transpired solar collector for air heating."
- [42] Ion V. Ion, J. G. M. (2006). "Design, developing and testing of a solar air collector."
- [43] Keith M. Gawlik, C. F. K. (2002). "Wind heat loss from corrugated, transpired solar collectors." Journal of Solar Energy Engineering.
- [44] L. H. Gunnewiek, E. B., K. G. T. Hollands (1996). "Flow distribution in unglazed transpired plate solar air heaters of large area."
- [45] L. H. Gunnewiek, K. G. T. H., E. Brundrett (2001). "Effect of wind on flow distribution in unglazed transpired-plate collectors."
- [46] Löffler, M. (2011). Verbesserung des Wirkungsgrades von Luftkollektoren durch Grenzschichtabsaugung, Simulationsergebnisse. Karlsruhe, Universität Karlsruhe.
- [47] M. Augustus Leon, S. K. (2006). "Mathematical modeling an thermal performance analysis of unglazed transpired solar collectors."
- [48] Romdhane, B. S. (2007). "The air solar collectors: comparative study, introduction of baffles to favor the heat transfer." Solar Energy **81**(1): 139-149.
- [49] S. J. Arulanandam, K. G. T. H., E. Brundrett (2000). "A CFD heat transfer analysis of the transpired solar collector under no-wind conditions."
- [50] Sadegh Motahar, A. A. A. (2010). "An Analysis of Unglazed Transpired Solar Collectors Based on Exergetic Performance Criteria."
- [51] Sébastien Cordeau, S. B. (2011). "Performance of unglazed solar ventilation air pre-heaters." ScienceDirect.
- [52] Shukla, A., D. N. Nkwetta, et al. (2012). "A state of art review on the performance of transpired solar collector." Renewable and Sustainable Energy Reviews **16**(6): 3975-3985.
- [53] Summers, D. N. (1995). "Thermal simulation and economic assessment of unglazed transpired collector systems."
- [54] T. N. Anderson, M. D., G. L. Morrison, J. K. Carson "Performance of a building integrated photovoltaic/thermal (BIPVT) solar collector."
- [55] V. Delisle, M. R. C. Model of a PV/thermal unglazed transpired collector.